

A PERSONAL OVERVIEW OF THE DEVELOPMENT OF PATCH ANTENNAS

Part 4

Kai Fong Lee

Dean Emeritus, School of Engineering and Professor
Emeritus, Electrical Engineering, University of Mississippi
and

Professor Emeritus, Electrical Engineering, University of
Missouri-Columbia

November 4, 2015

City University of Hong Kong

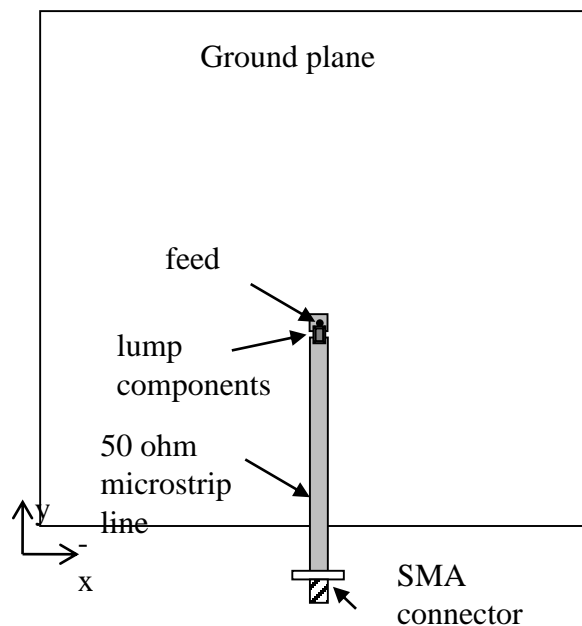
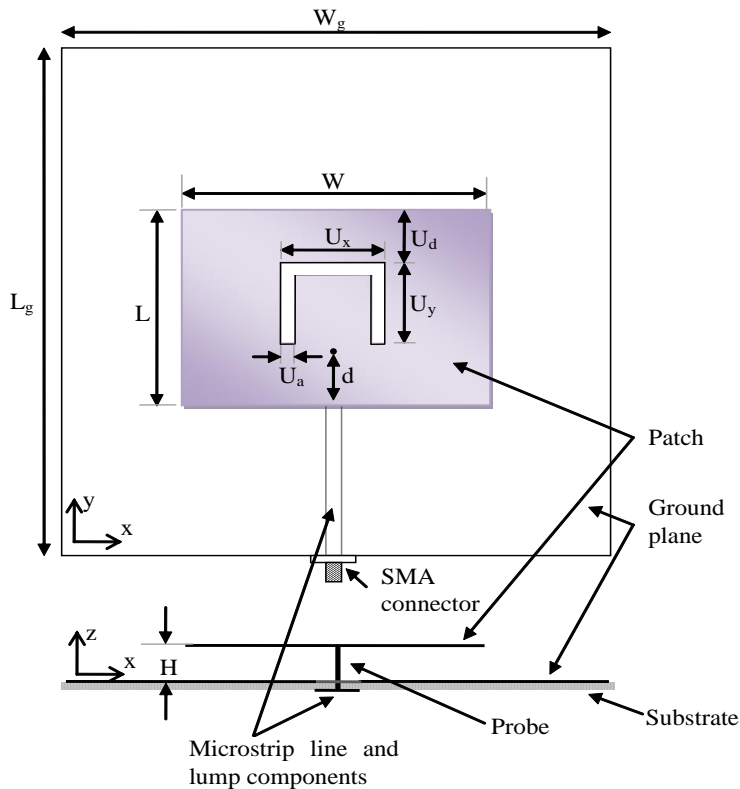
Schedule

Part 1 (Hour 1)	Part 2 (Hour 2)	Part 3 (Hour 3)	Part 4 (Hour 4)
1. How I got into patch antenna research	5. Broadbanding techniques	7. Dual/triple band designs	9. Reconfigurable patch antennas
2. Basic geometry and basic characteristics of patch antennas	6. Full wave analysis and CAD formulas	8. Designs for circular polarization	10. Size reduction techniques
3. Our first topic			11. Concluding remarks and some citation data
4. Our research on topics related to basic studies			

9. Reconfigurable Patch Antennas

There are three main kinds of reconfigurable patch antennas: pattern reconfigurable, frequency reconfigurable, and polarization reconfigurable. The patch antenna with adjustable air gap discussed in part 1 is an example of a frequency reconfigurable antenna, which was the first problem we worked on. In 2008, Steven Yang, myself and Prof. A. Kishk published a paper on frequency reconfigurable U-slot patch antenna. Several years later, Ahmed Khidre, Prof. A. Elsherbeni and myself published a paper on the Polarization Reconfigurable E-Shaped Patch Antenna

9.1 Frequency Reconfigurable U-slot Patch Antenna (Yang et al. 2008)



Geometry of the tuning circuit (back side of the antenna)

Fig. 4.1 Geometry of the frequency tunable U-slot patch antenna. Dimensions: $W=77\text{mm}$, $L=57\text{mm}$, $H=12\text{mm}$, $U_x = 32\text{mm}$, $U_y = 31\text{mm}$, $U_a = 2\text{mm}$, $U_d = 14.5\text{mm}$, $d=26\text{mm}$, Ground plane $150\text{mm} \times 150\text{mm}$. Microstrip line is fabricated on substrate of dielectric constant 2.6 and thickness 1.524 mm. Trimmer has a capacitance range between 0.4 and 1.5 pF. A chip inductor of 1 nH is connected in parallel to the trimmer.

9.1 Frequency Reconfigurable U-slot Patch Antenna

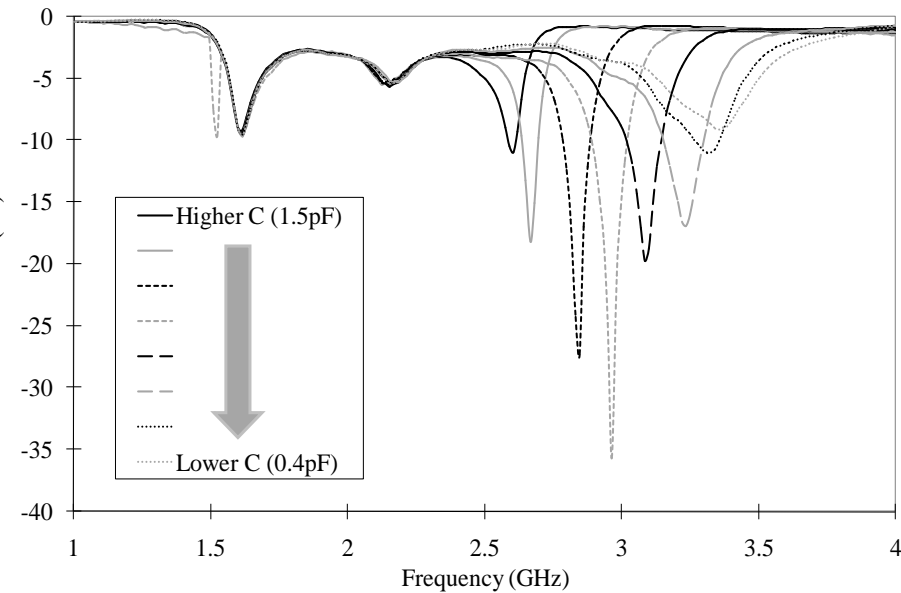


Fig. 4.2 Measured return loss with different capacitance value obtained by rotating the trimmer

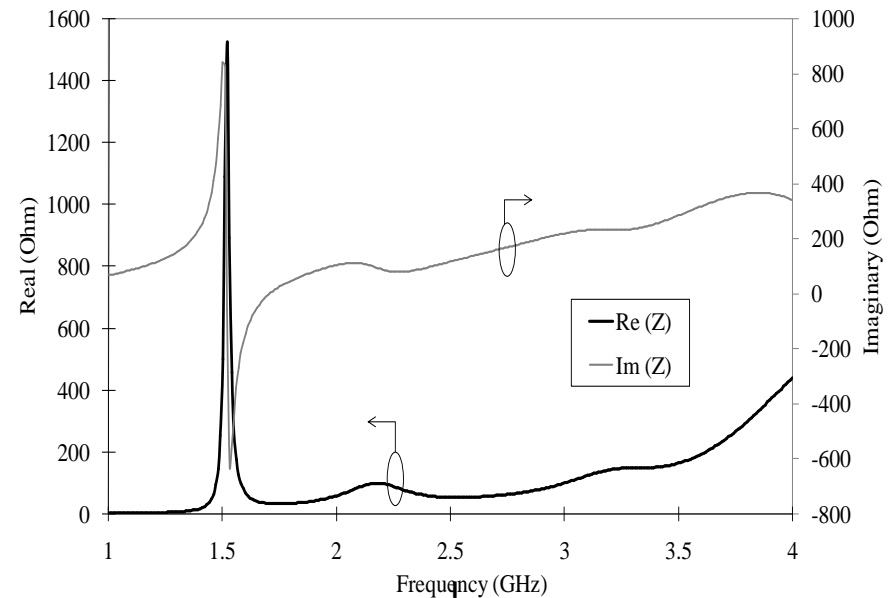


Fig. 4.3 Input impedance of U-slot patch antenna without lumped components

Observations:

By changing the capacitance of the trimmer, the frequency can be tuned from 2.6 to 3.35 GHz.

Note that the input impedance of the U-slot patch without lumped components is quite different from the regular patch without the U-slot. The input resistance is relatively flat and the input reactance relatively linear.

In the experiment, the parameters were chosen such that the tuning frequency range is outside the broadband range (about 1.5 GHz to 2.4 GHz). The broadband range was not matched. Perhaps with further optimization, the broadband range can be matched as well.

9.2 Polarization Reconfigurable E-Shaped Patch Antenna

9.2.1 Introduction

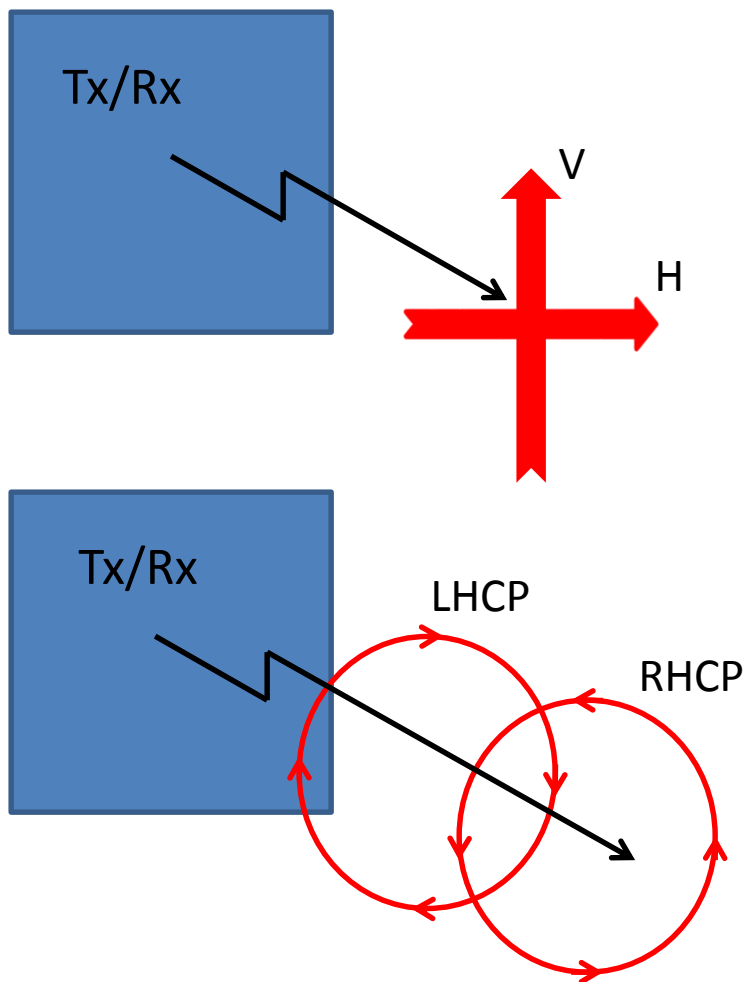
9.2.2 Principle of operation

9.2.3 Prototype and Results

9.2.4 Conclusions

9.2.1 Introduction

Polarization agile antenna??  Alter its polarization characteristics.



Linear polarization agility

Changing field from Vertical to Horizontal or the opposite.

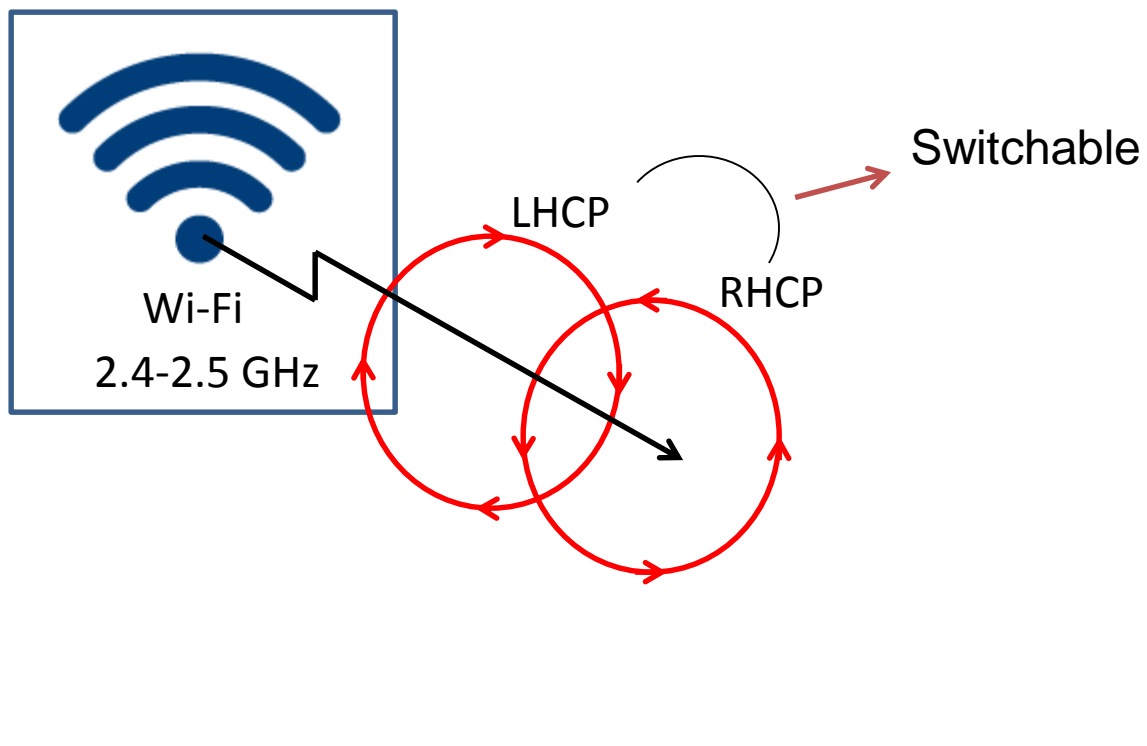
Circular polarization agility

Changing from LHCP to RHCP or the opposite.

Advantages

- Increase system capacity via frequency reuse.
- Diversity in Tx/Rx link.
- One antenna roam to different wireless systems.
- Compactness of wireless devices.

Goal



- Designing microstrip antenna with switchable LHCP/RHCP that covers 2.4-2.5GHz band (4%) for Wi-Fi application.

CP E-Shaped Patch Antenna

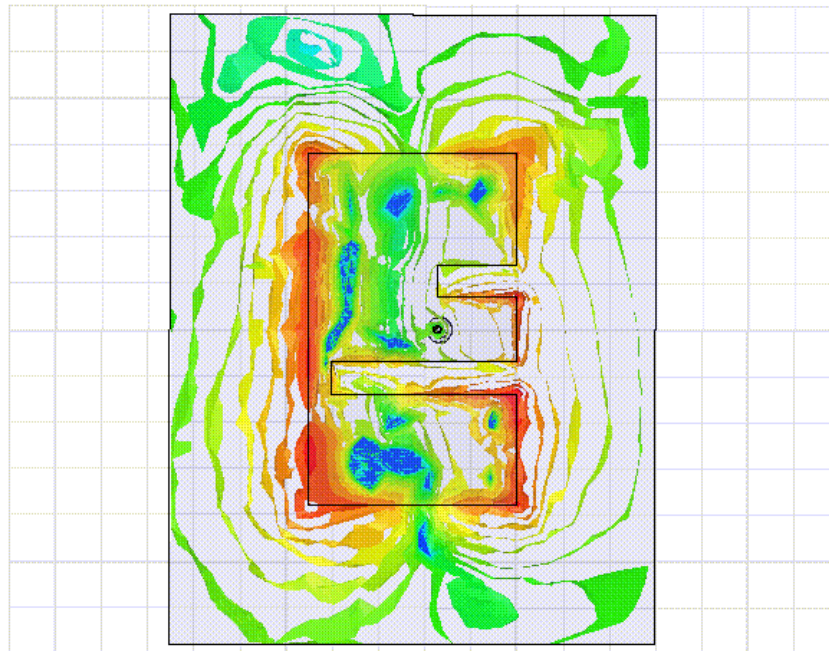
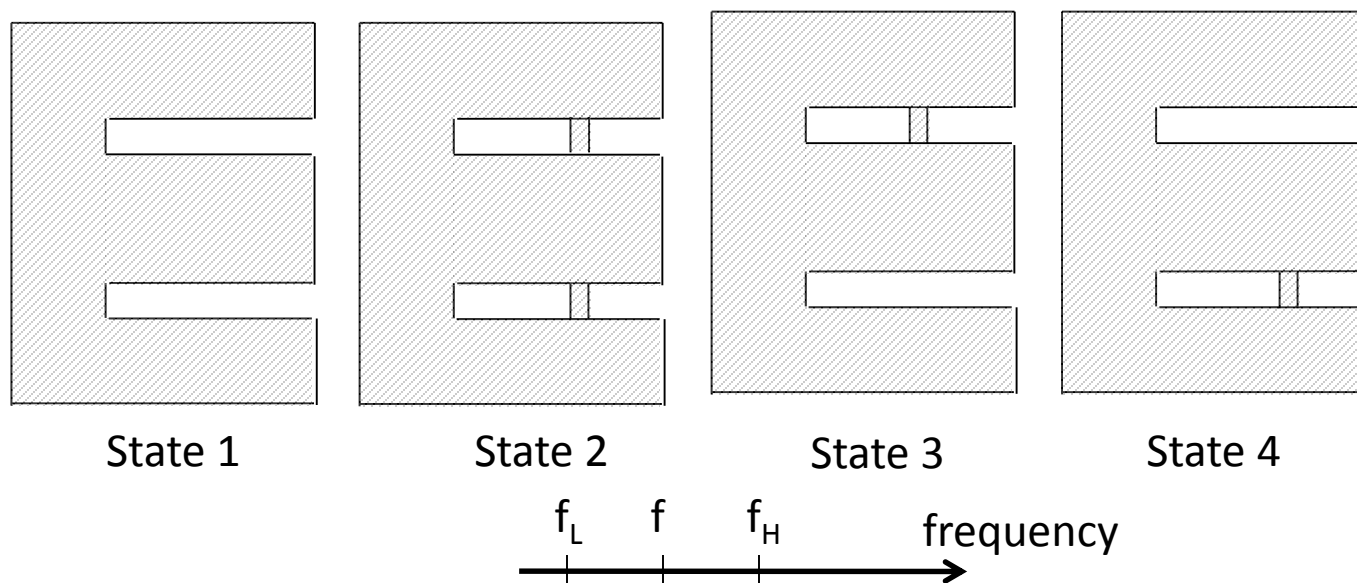


Fig. 4.4 E-shaped patch with unequal slots gives wide band circularly polarized characteristics (-10 dB S_{11} , 3 dB axial ratio $>4\%$ bandwidth).

Ahmed Khidre, Kai-Fong Lee, Fan Yang, and Atef Elsherbeni, "Wide Band Circularly Polarized E-shaped Patch Antenna For Wireless Applications," *IEEE Antennas Propag. Mag.*, vol. 52, no. 5, pp. 219-229, October 2010.

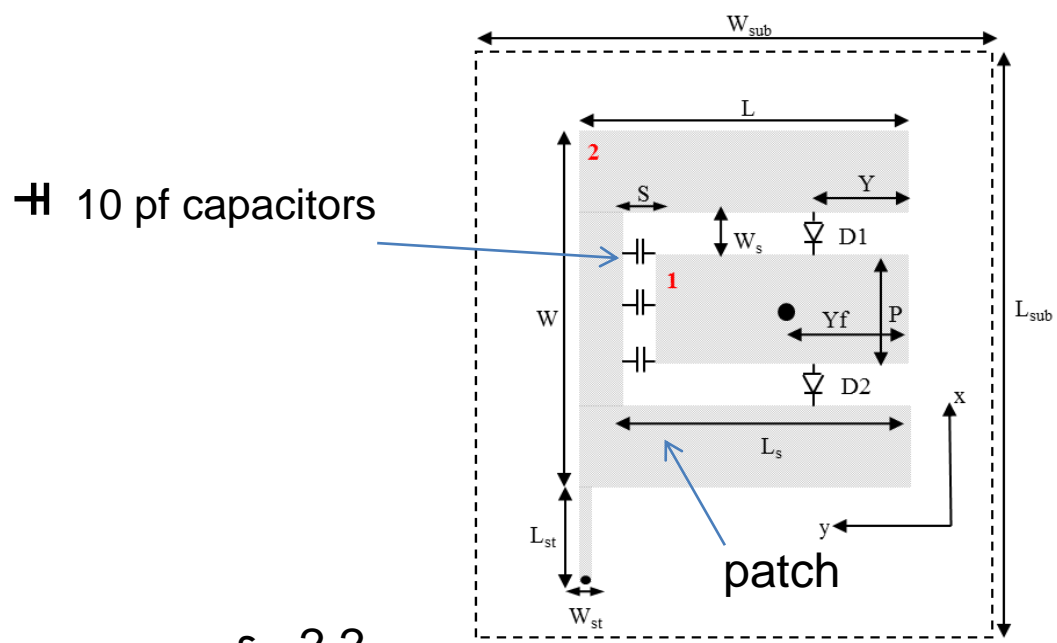
9.2.2 Principle of operation



State	Switch 1	Switch 2	Frequency	Polarization
1	OFF	OFF	f_L	LP
2	ON	ON	f_H	LP
3	ON	OFF	f	LHCP
4	OFF	ON	f	RHCP

Fig. 4.5 Illustrating four states of polarization

9.2.3 Prototype and results



⊕ 10 pf capacitors

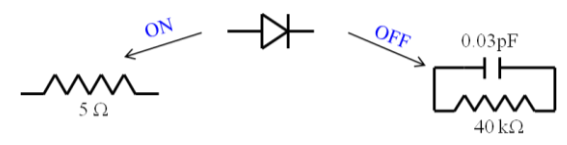


Fig. 4. The linear circuit model of the PIN diode (MA4SPS402) in both ON and OFF states used in full wave simulation

$\epsilon = 2.2$

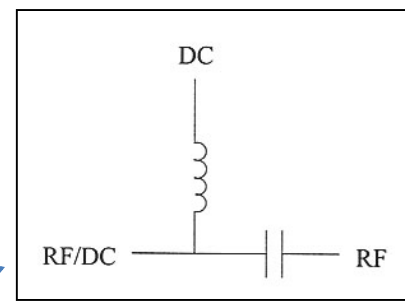
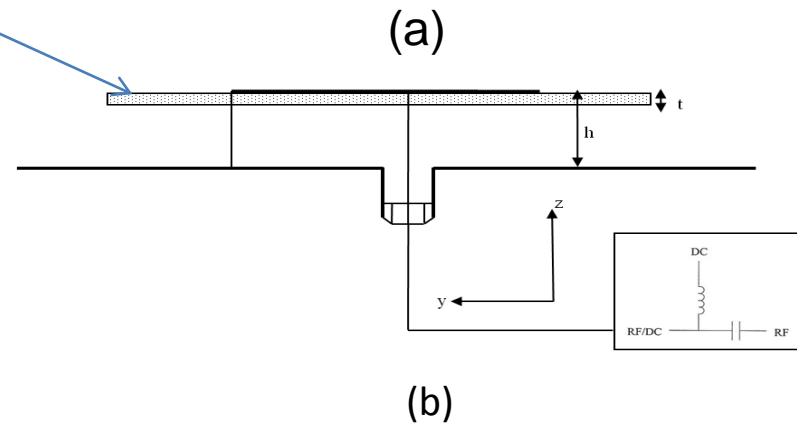


Fig. 4.6 Geometry of a single-feed reconfigurable E-shaped patch antenna with integrated DC biasing circuit: (a) top view; (b) side view: $L_{sub} = 140\text{mm}$, $W_{sub} = 80\text{mm}$, $L = 43\text{mm}$, $W = 77\text{mm}$, $L_s = 30\text{mm}$, $W_s = 7\text{mm}$, $P = 17\text{mm}$, $Y_f = 14\text{mm}$, $L_{st} = 28\text{mm}$, $W_{st} = 0.3\text{mm}$, $S = 0.5\text{mm}$, $h = 10\text{mm}$, $t = 0.787\text{mm}$.

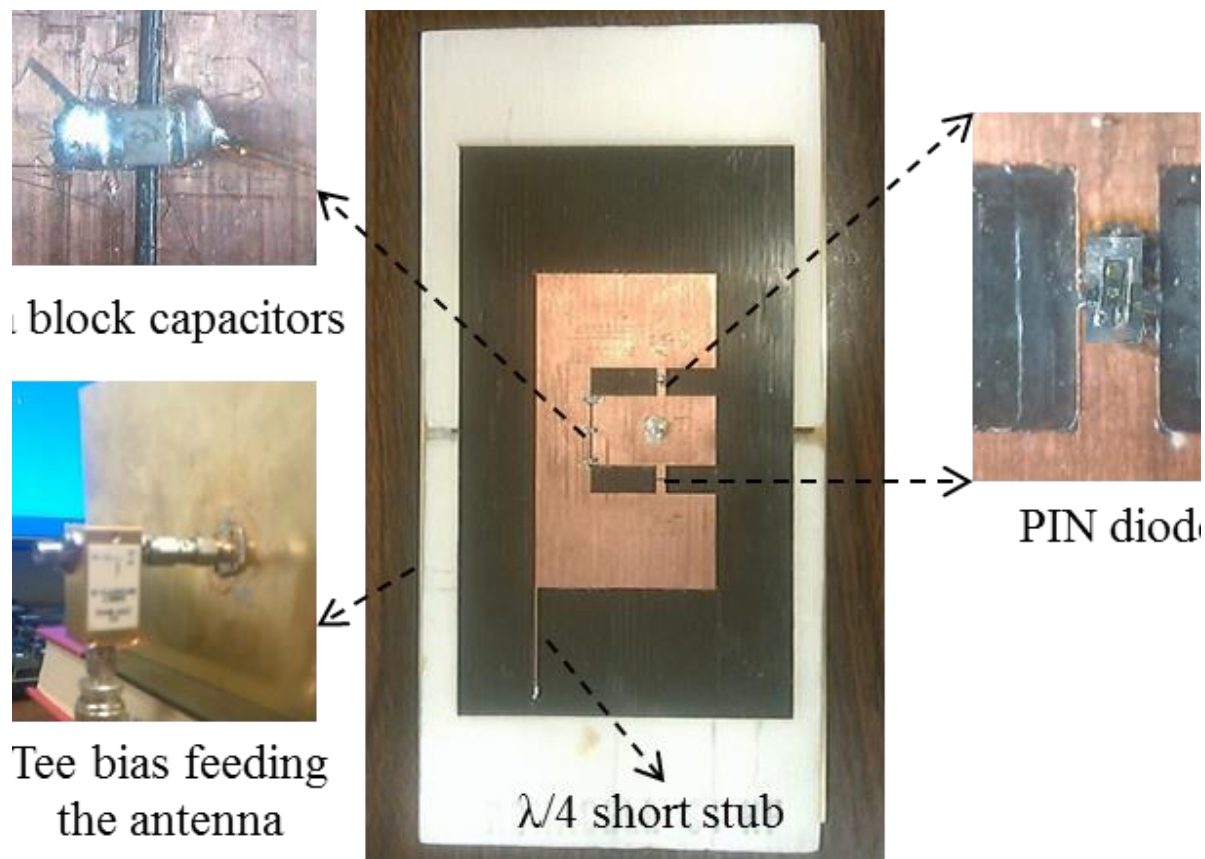
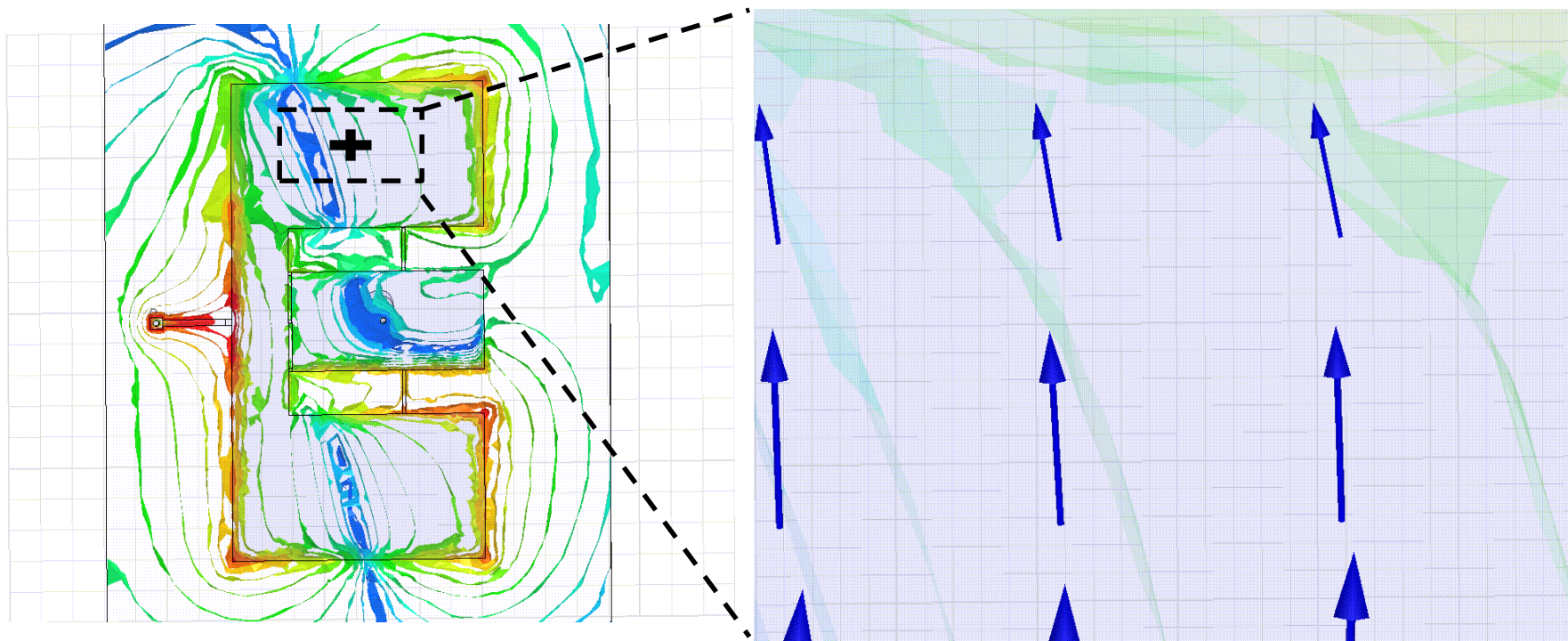


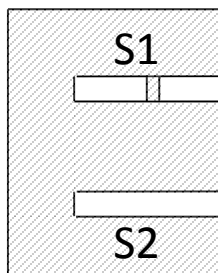
Fig. 4.7 Photo of polarization reconfigurable E-shaped patch antenna prototype along with the associated switching and biasing assemblies

Field Animation Beneath the Patch at State 3



LHCP Field distribution beneath the E-patch

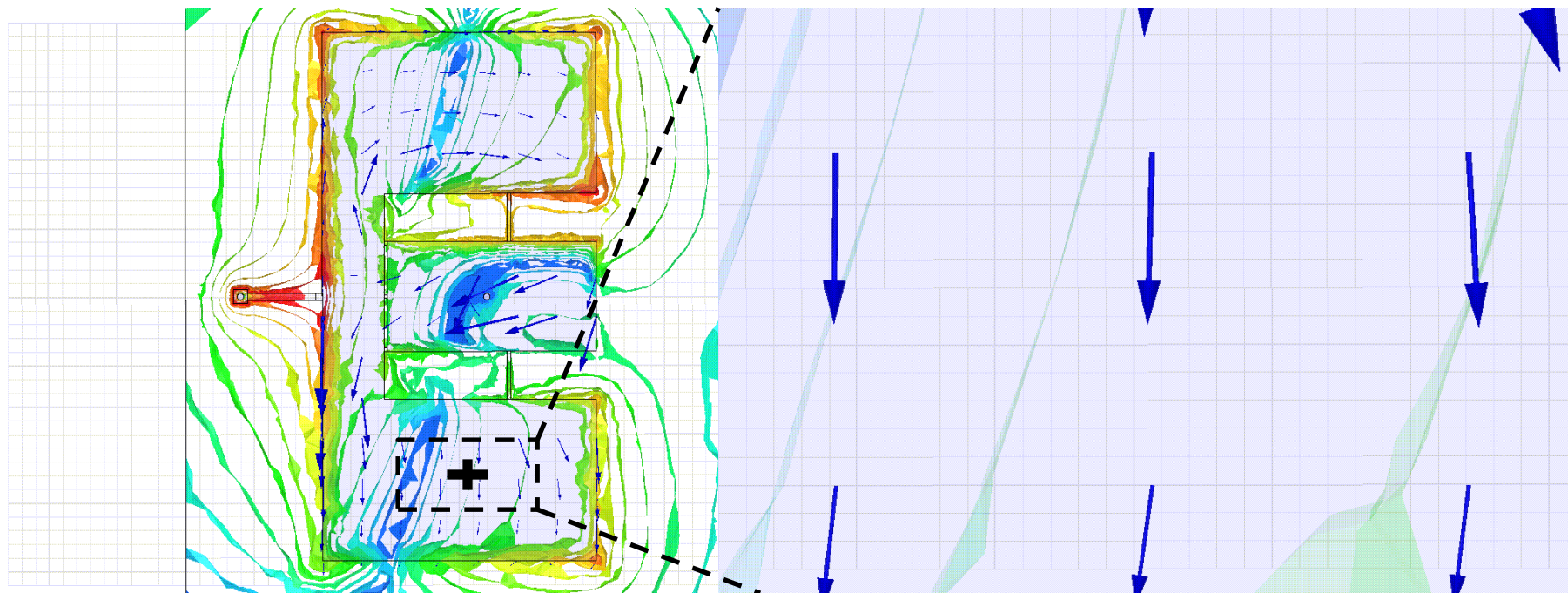
LHCP Zoomed Current vector distribution



Switch 1 ON

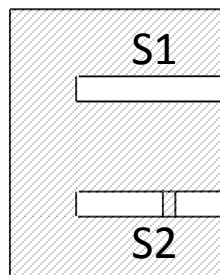
Switch 2 OFF

Field Animation Beneath the Patch at State 4



RHCP Field distribution beneath the E-patch

RHCP Zoomed Current vector distribution



Switch 2 ON
Switch 1 OFF

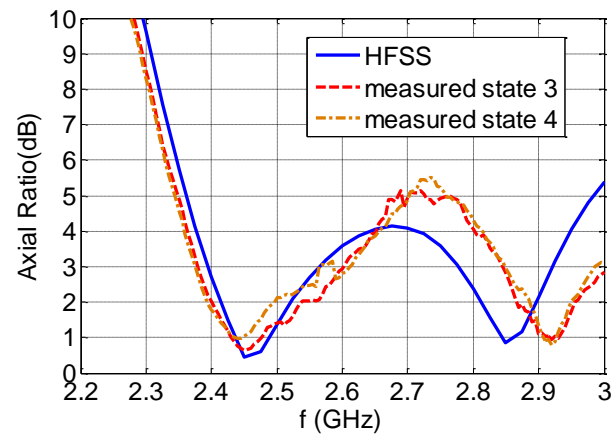
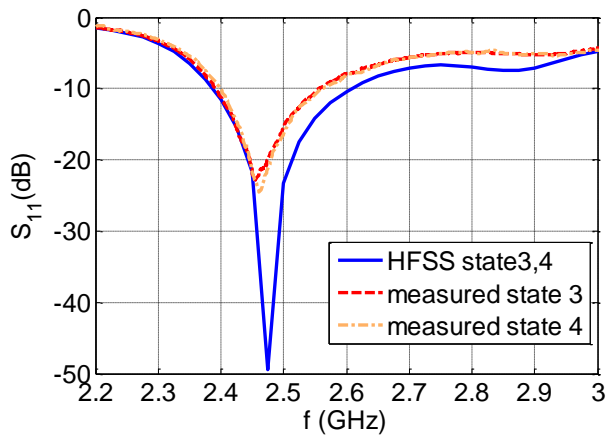


Fig. 4.8 Reflection coefficient and axial ratio of the prototype CP E-shaped patch antenna

Quantity	SIMULATION	MEASURED
$S_{11} (< -10dB)$	2.39-2.6 GHz (8.4%)	2.4-2.575 GHz (7%)
<i>Axial ratio</i> (<3dB)	2.4-2.6 GHz (8%)	2.38-2.6GHz (8.8%)

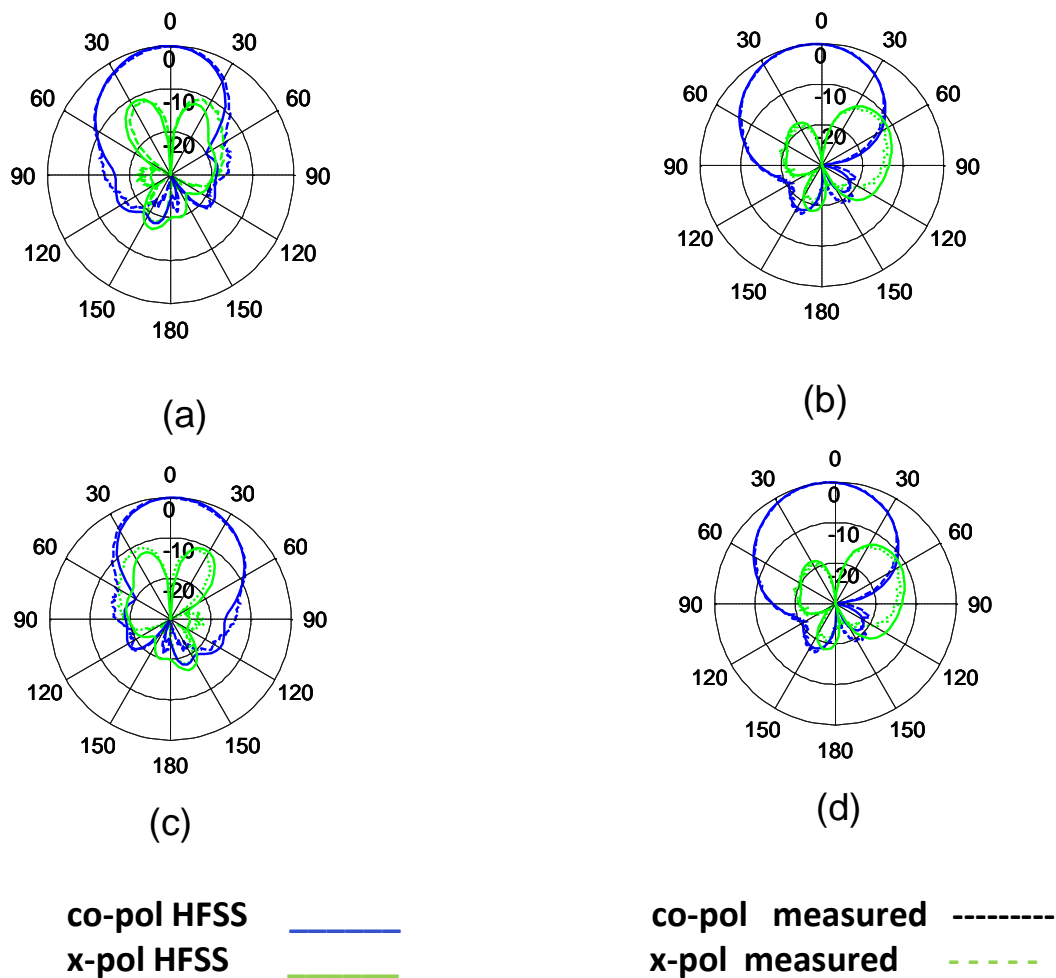


Fig. 4. 9 Simulated and measured radiation pattern of the prototype antenna at 2.45 GHz: (a) x-z plane at state 3; (b) y-z plane at state 3; (c) x-z plane at State 4; and (d) y-z plane at state 4.

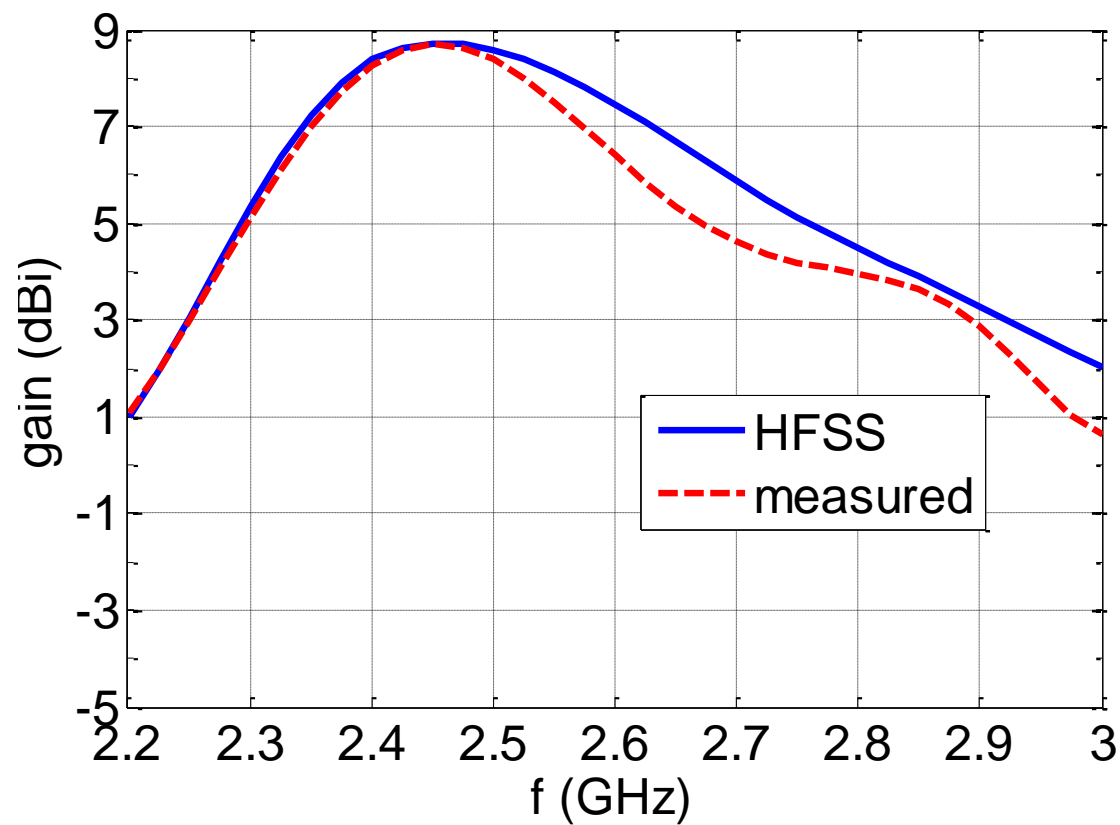


Fig. 4.10 Gain of the CP E-shaped patch antenna

Conclusion

- Polarization reconfigurable E-shaped patch antenna is proposed which exhibits effective bandwidth $\sim 6.5\%$ and design simplicity (few parameters to be optimized).
- Proposed design is a good candidate for the implementation of polarization agile antenna for wireless applications such as WLAN, Wi-Max.



References for reconfigurable patch antennas

K. F. Lee, K. Y. Ho and J. S. Dahele, Circular-disc microstrip antenna with an air gap, *IEEE Transactions on Antennas & Propagation*, Vol. 32, 880-884, 1984.

S.L.S. Yang, A.A. Kishk, K.F. Lee, "Frequency Reconfigurable U-slot Microstrip Patch Antenna," *IEEE Antennas and Wireless Propagation Letters*, Vol. 7, pp. 127-129, 2008.

A. Khidre, K. F. Lee, F. Yang and A. Z. Elsherbeni, "Circular polarization Reconfigurable wideband E-shaped patch antenna for wireless applications, *IEEE Transactions on Antennas and Propagation*, Vol. 61, No. 2, pp. 960-964, 2013.

10. SIZE REDUCTION TECHNIQUES

- 10.1 Summary
- 10.2 Use of shorting wall – the quarter wave patch
 - 10.2.1 Introduction
 - 10.2.2 Formula for resonant frequency
 - 10.2.3 Experimental results
 - 10.2.4 Partially shorted patch and Planar Inverted F Antenna (PIFA)
- 10.3 Use of shorting pin
- 10.4 The folded patch
- 10.5 Small-size wide bandwidth patch antennas
- 10.6 Comments on ground plane size effect

10.1 Summary

In many applications, it is desirable for the dimensions of the patch to be small fractions of the free space wavelength. The resonant length of the patch antenna is approximately $\lambda/2$, where λ is wavelength in the dielectric substrate. It follows that the size of the patch can be reduced by using high dielectric constant. However, the resulting patch antenna will have narrow impedance bandwidth. This motivates the search for other size reduction methods.

By placing a shorting wall along the null in the electric field across the center of the patch, the resonant length can be reduced by a factor of two (Pinhas & Shtrikman 1988; Chair et al. 1999; Lee et al. 2000). The area occupied by the patch will be reduced by a factor of four, if the aspect ratio is kept the same.

Another technique to reduce the resonant length is to add a shorting pin in close proximity to the feed (Waterhouse et al. 1998). The shorting pin is capacitively coupled to the resonant circuit of the patch, effectively increasing the permittivity of the substrate. It has been shown that a suitably placed shorting pin can reduce the resonant length of a circular patch by a factor of three, and the area of the patch by a factor of nine. Broadbanding techniques such as stacked patches, U-slot patch, and L-probe fed can be applied to obtain small size wideband patch antennas (Shackelford et al. 2003). All these methods result in radiation patterns with high cross polarization. This may not be a disadvantage in indoor mobile communication applications. A low cross polarization design is that of the folded patch, which, however, is thicker and more difficult to fabricate (Luk, Chair, and Lee 1998).

The above methods were originally developed for linearly polarized patch antennas. Suitably modified, they can also be applied to reduce the patch size of circularly polarized patch antennas. A recent review article (Wong et al. 2012) presents a comprehensive account of small antennas in wireless communications, which include some methods not mentioned above.

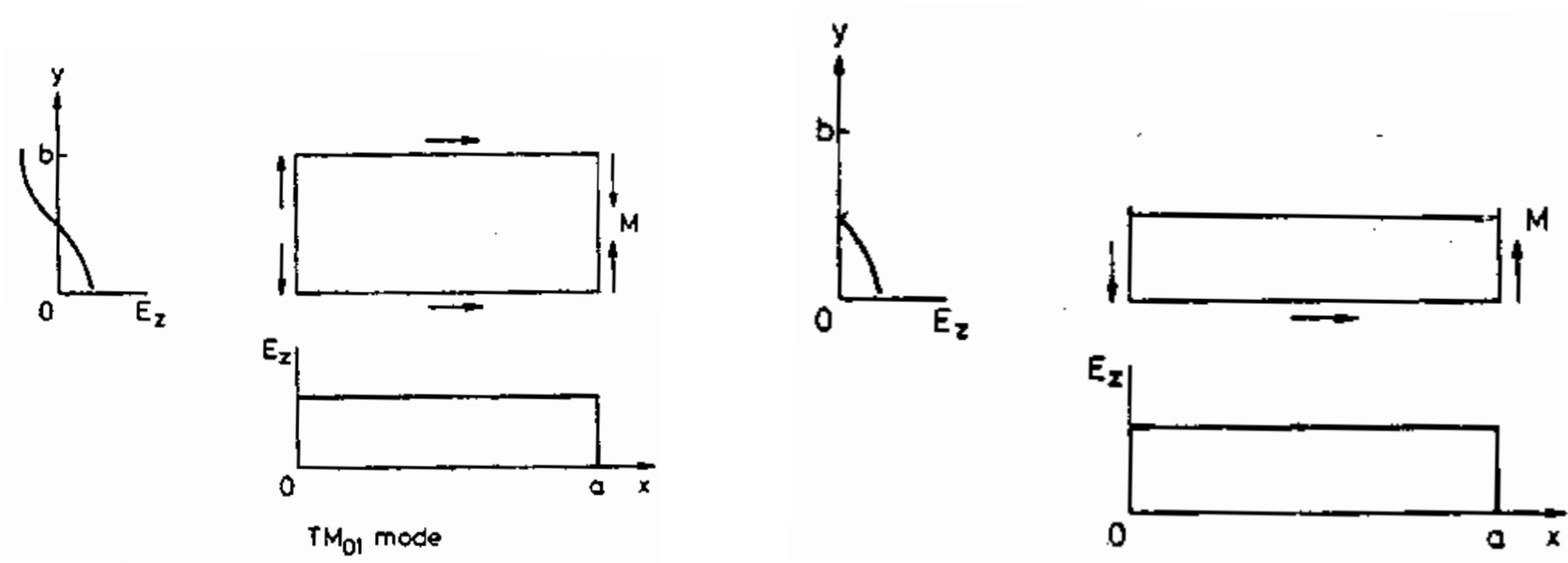
10.2 Use of Shorting Wall – Quarter Wave Patch

10.2.1 Introduction

- The electric field distributions under the patch for the TM_{01} and TM_{10} modes have a null along the center of the patch. The fields are not perturbed when a short is placed at the null line. This results in a shorted quarter-wave patch, with the same resonant frequency as the regular half-wave patch. For the same aspect ratio, the area of the quarter wave patch is four times smaller than the half-wave patch, as illustrated in Fig.4.11.

10.2 Use of Shorting Wall – Quarter Wave Patch

10.2.1 Introduction



(a) Regular half-wave patch

(b) Shorted quarter-wave patch

Fig. 4.11 Electric field distributions of (a) regular half-wave patch and (b) shorted quarter-wave patch.

10.2 Use of Shorting Wall – Quarter Wave Patch

10.2.2 Formula for Resonant Frequency

- Consider the rectangular cavity representing the shorted patch shown in Fig.4.12, where the side wall $y = 0$ is shorted. Thus $\mathbf{E}_t = 0$ at $y = 0$ as well as on the top and bottom, while $\mathbf{H}_t = 0$ on the other three side walls.

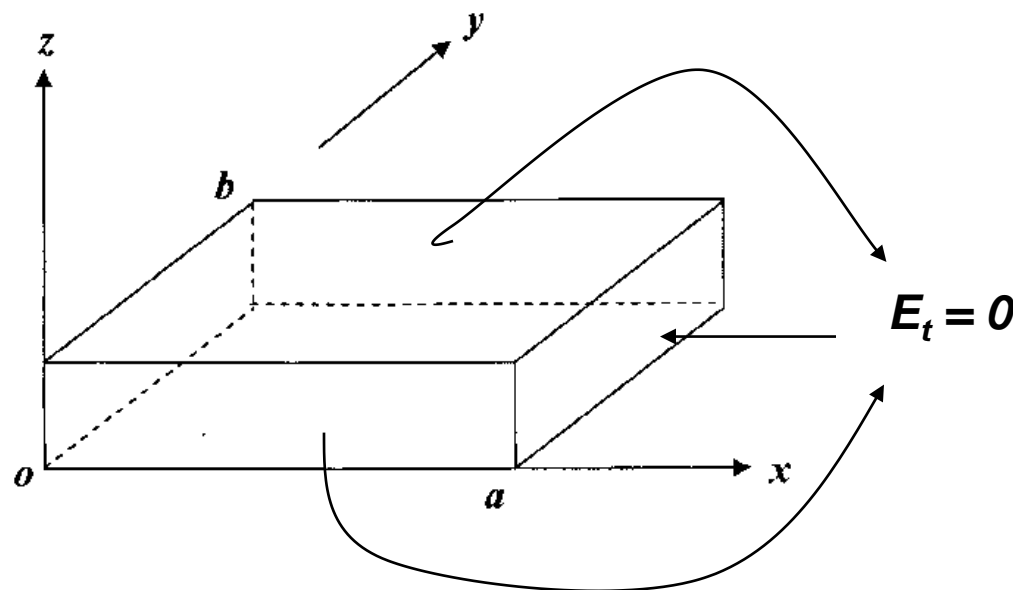


Fig. 4.12 Geometry of the shorted patch.

10.2 Use of Shorting Wall – Quarter Wave Patch

10.2.2 Formula for Resonant Frequency

- The solution $\nabla^2 E_z + k_d^2 E_z = 0$ satisfying the boundary conditions is: for

$$E_z = E_0 \cos\left(\frac{m\pi}{a} x\right) \sin\left(\frac{(2n-1)\pi}{2b} y\right)$$

- The eigenvalues for k_d^2 are given by

$$k_{mn}^2 = \left(\frac{m\pi}{a}\right)^2 + \left(\frac{(2n-1)\pi}{2b}\right)^2$$

10.2 Use of Shorting Wall – Quarter Wave Patch

10.2.2 Formula for Resonant Frequency

- The resonant frequencies are therefore given by:

$$f_{nm} = \frac{c}{2\sqrt{\epsilon_r}} \sqrt{\left(\frac{m}{a}\right)^2 + \left(\frac{2n-1}{2b}\right)^2}, \quad c = \frac{1}{\sqrt{\mu_0 \epsilon_0}}$$

- The lowest mode is **TM_{00}** :

$$f_{00} = \frac{c}{4b\sqrt{\epsilon_r}} \quad \text{or} \quad b = \frac{\lambda_{00}}{4\sqrt{\epsilon_r}} \quad \text{where} \quad \lambda_{00} = \frac{c}{f_{00}}$$

- This is to be compared with

$$b = \frac{\lambda_{01}}{2\sqrt{\epsilon_r}} \quad \text{where} \quad \lambda_{01} = \frac{c}{f_{01}} \quad \text{for the rectangular patch.}$$

10.2 Use of Shorting Wall – Quarter Wave Patch

10.2.2 Formula for Resonant Frequency

- Hence, to resonate at the same frequency, the length b for the shorted patch is half that of the regular patch. The shorted patch is known as the quarter-wave patch while the regular patch is known as the half-wave patch.
- Based on cavity model, the various antenna characteristics of the shorted patch can be calculated following the procedures used for the regular patch. For brevity, the detailed theoretical results are not presented here.

10.2 Use of Shorting Wall – Quarter Wave Patch

10.2.3 Experimental Results

- Chair et al. [1999] presented experimental results of the quarter-wave patch shown in Fig.4.13. The substrate between the patch and the ground plane is foam, with thickness h and relative permittivity 1.08. The sides of the patch are $a = b = 3.06$ cm long, with one side shorted. The patch is fed by a coaxial probe, with the feed point at $x = 0$, $y = d$, where d is the distance between the feed point and the open edge and is adjusted for best match.
- Pattern and bandwidth (VSWR = 2) measurements were performed for several thicknesses h . The results for bandwidth are summarized in table 4.1.

10.2 Use of Shorting Wall – Quarter Wave Patch

10.2.3 Experimental Results

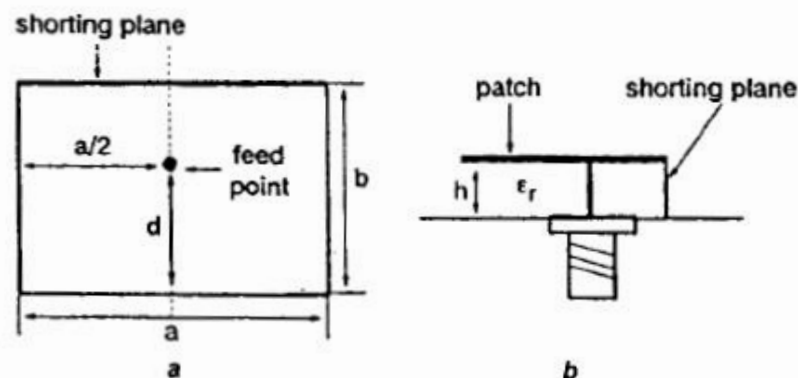


Fig. 4.13 Geometry of shorted patch.

(a) Top view; (b) Side view.

Table 4.1 Bandwidth Measurements.

Case	h (mm)	d (mm)	Quarter-Wave Patch		d (mm)	Half-Wave Patch	
			BW (%)	Center Frequency (GHz)		BW (%)	Center Frequency (GHz)
a	2	22	3.59	2.194	23	1.57	2.225
b	3	23	4.73	2.061	23	2.30	2.175
c	4	20	6.40	2.11	23	2.60	2.115
d	5	17	9.69	2.166	20	3.55	2.115
e	6	5	17.39	2.566	18	4.66	2.125
f	7	5	17.66	2.462	15	5.55	2.16

10.2 Use of Shorting Wall – Quarter Wave Patch

10.2.3 Experimental Results

- It is noted in table 4.1 that the shorted patch on foam substrate has relatively wide bandwidth. For $h = 7$ mm, which corresponds to about $0.058 \lambda_0$ at the center frequency, the impedance bandwidth is 18.54 %. For comparison, for a half-wave regular patch of the same thickness and the same width but double in length, the measured impedance bandwidth, as shown in table 4.2, was found to be only 5.55 %. Comparisons with calculations are in qualitative agreement and are shown in tables 4.2 (a) and 4.2 (b). The shorted patch has a smaller volume and therefore less stored energy, leading to a smaller Q and larger bandwidth.
- For material substrates, Lee et al. [2000] showed that the BW of the shorted patch is less than the regular patch. This is due to the fact that there are surface waves in the substrate. This loss is larger for the regular patch, leading to a smaller Q and larger bandwidth.

10.2 Use of Shorting Wall – Quarter Wave Patch

10.2.3 Experimental Results

Table 4.2 (a). Resonant frequencies and bandwidth of the shorted square patch of Fig. 13.3 with $a = b = 3.06$ cm and $\epsilon_r = 1.08$.

h (mm)	d/b	Experiment		Calculation	
		f_0 (GHz)	BW (%)	f_0 (GHz)	BW (%)
2	0.72	2.19	3.59	2.19	1.8
3	0.75	2.06	4.73	2.13	4.2
4	0.65	2.11	6.40	2.13	6.3
5	0.56	2.17	9.70	2.17	8.6
6	0.16	2.57	14.0	2.54	12.7
7	0.16	2.46	17.7	2.49	16.4

10.2 Use of Shorting Wall – Quarter Wave Patch

10.2.3 Experimental Results

Table 4.2 (b). Resonant frequencies and bandwidth of the regular rectangular patch of Fig. 13.3 with $a = 3.06$ cm, $b = 6.12$ cm and $\epsilon_r = 1.08$.

h (mm)	d/b	Experiment		Calculation	
		f_0 (GHz)	BW (%)	f_0 (GHz)	BW (%)
2	0.75	2.20	3.2	2.23	1.57
3	0.75	2.16	3.7	2.18	2.30
4	0.75	2.14	3.75	2.12	2.60
5	0.65	2.15	5.3	2.12	3.55
6	0.59	2.16	6.3	2.13	4.66
7	0.49	2.20	7.3	2.16	5.55

- The measured E and H plane patterns at the center frequency for each of the six cases in table 4.2 are shown in Figs.4.14 (a) – (f). The measurements are made with the feed positions indicated.

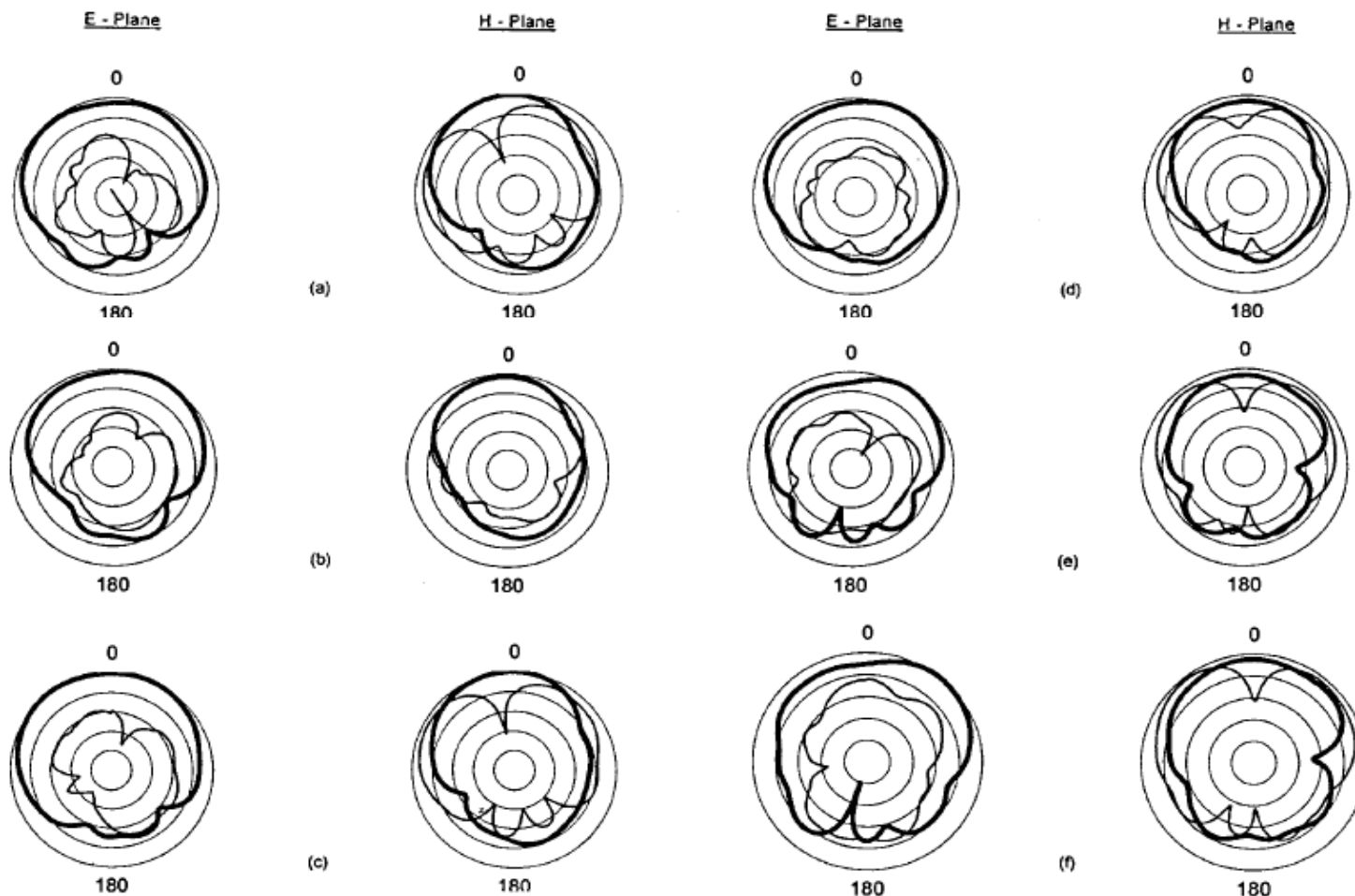


Fig. 4.14 Copolarization and cross-polarization patterns at the center frequencies for the six cases shown in Table 4.2. Copol, x-pol, 10 dB/div.

10.2 Use of Shorting Wall – Quarter Wave Patch

10.2.3 Experimental Results

- The measured patterns show large cross polarizations in the E -plane. They also show that, depending on the thickness, the maximum radiation can occur off broadside. The gain values (Lee et al. 2000) at the resonant frequencies are summarized in table 13.3. It is seen that typical values of the maximum gain are in the range 2-3.5 dBi. This is about half of the regular half-wave patch.

10.2 Use of Shorting Wall – Quarter Wave Patch

10.2.3 Experimental Results

Table 4.3 Measured gain of the shorted square patch of Fig.

13. 3.

h (mm)	f_0 (GHz)	Gain (dBi)	
		broadside	maximum direction θ^*
3	2.06	2.5	2.5 at 0°
5	2.17	2.5	3.5 at 30°
7	2.46	0.2	2.2 at 45°

θ^* is measured from the perpendicular direction in the E -plane (perpendicular to the shorting plane).

10.2.4 Partially Shorted Patch and Planar Inverted F Antenna

- Figure 4.15 shows the geometry in which the shorting wall, instead of extending fully across the width of the patch \mathbf{a} , has a width \mathbf{s} , where $\mathbf{s} \leq \mathbf{a}$. It was shown in Hirasawa and Haneishi (1992) that the use of a partially shorted wall had the effect of reducing the resonant frequency of the antenna. Lee et al. (2000) showed that this was accompanied at the expense of bandwidth. Their calculated results are shown in Fig. 4.15 for an antenna with $\mathbf{a} = 3.8$ cm, $\mathbf{b} = 2.5$ cm, $\mathbf{h} = 3.2$ cm and $\epsilon_r = 1.0$. It is seen that, as \mathbf{s}/\mathbf{a} decreases from 1.0 to 0.1, the resonant frequency decreases from 2.69 to 1.61 GHz, representing a 60 % reduction in frequency or size. However, this is accomplished at the expense of bandwidth, which is reduced from 7.4 % for $\mathbf{s}/\mathbf{a} = 1.0$ to 3.7 % for $\mathbf{s}/\mathbf{a} = 0.1$.

10.2.4 Partially Shorted Patch and Planar Inverted F Antenna

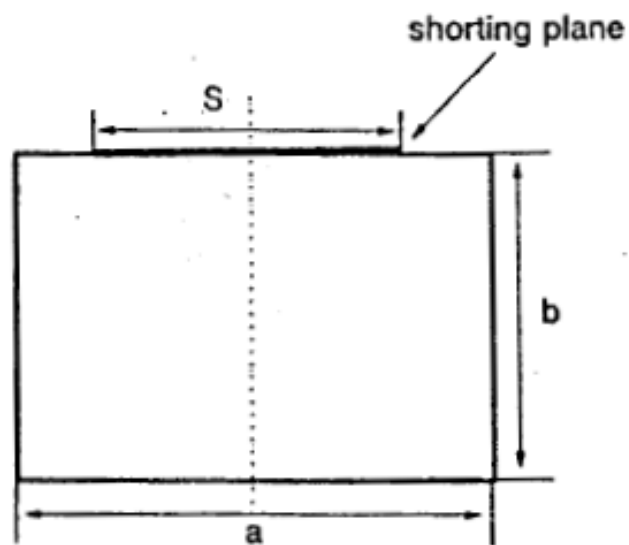


Fig. 4.15 Geometry of partially shorted patch.

10.2.4 Partially Shorted Patch and Planar Inverted F Antenna

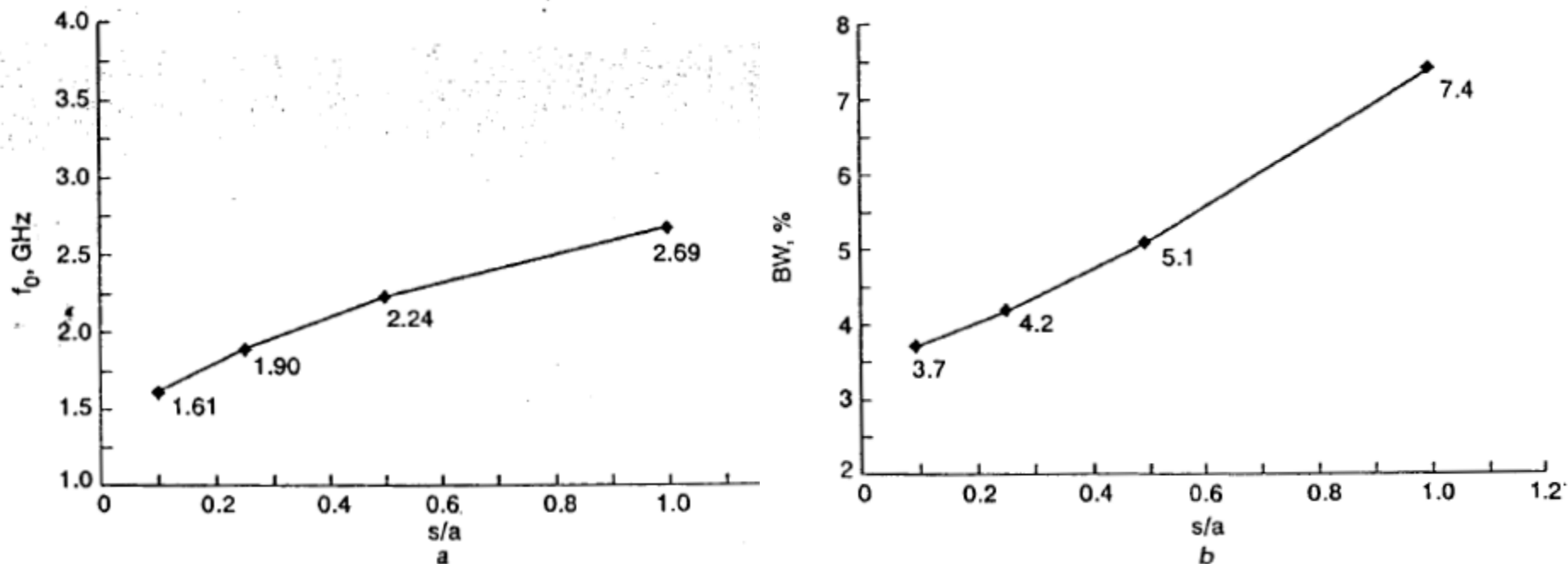


Fig. 4.16 Calculated resonant frequency and bandwidth of partially shorted with $a = 3.8$ cm, $b = 2.5$ cm on foam substrate ($\epsilon_r = 1$) of thickness $h = 3.2$ mm.

- (a) Resonant frequency
- (b) Bandwidth

10.2.4 Partially Shorted Patch and Planar Inverted F Antenna

- The partially shorted patch in the form shown in Fig. 4.17 is known as the planar inverted F antenna (PIFA), because the side view looks like an inverted F. The width of the shorting wall w is approximately $0.2 L_1$ while the dimensions of L_1 , and L_2 are on the order of $1/8 \lambda_0$.

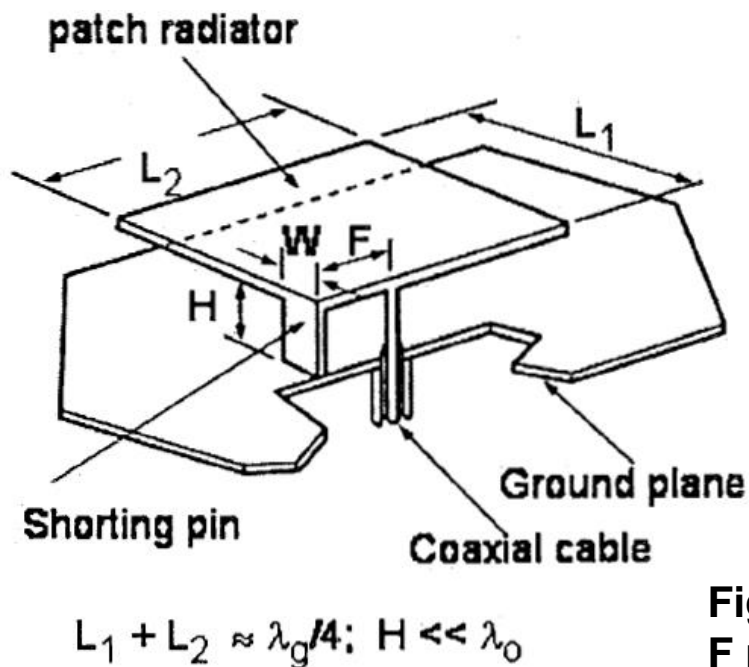


Fig. 4.17 Size reduction by using an inverted-F patch.

10.3 Use of Shorting Pin

- Another technique for reducing the patch size, very similar to the inverted-F method, is to use a shorting pin (Waterhouse et al. 1998). This is illustrated in Fig.4.18. Both the shorting plate and the shorting pin cause the fields underneath the patch to bounce back-and-forth. The field starts to radiate once the bouncing distance reaches half-wavelength. As a result of the multiple bounces, the physical size of the patch is reduced. Since the bounces are non-unidirectional, the fields can radiate out from almost all edges of the patch, resulting in high cross-polarization. However, for certain applications such as cellular phone communication in a multi-path environment, high cross-polarized fields is not a concern.
- If the shorting pin is close to the feed, the resonant circuit of the patch is capacitively coupled to the pin. This is equivalent to increasing the permittivity of the substrate, which further contributes to reduction in frequency or size of the patch (measured in wavelength).

10.3 Use of Shorting Pin

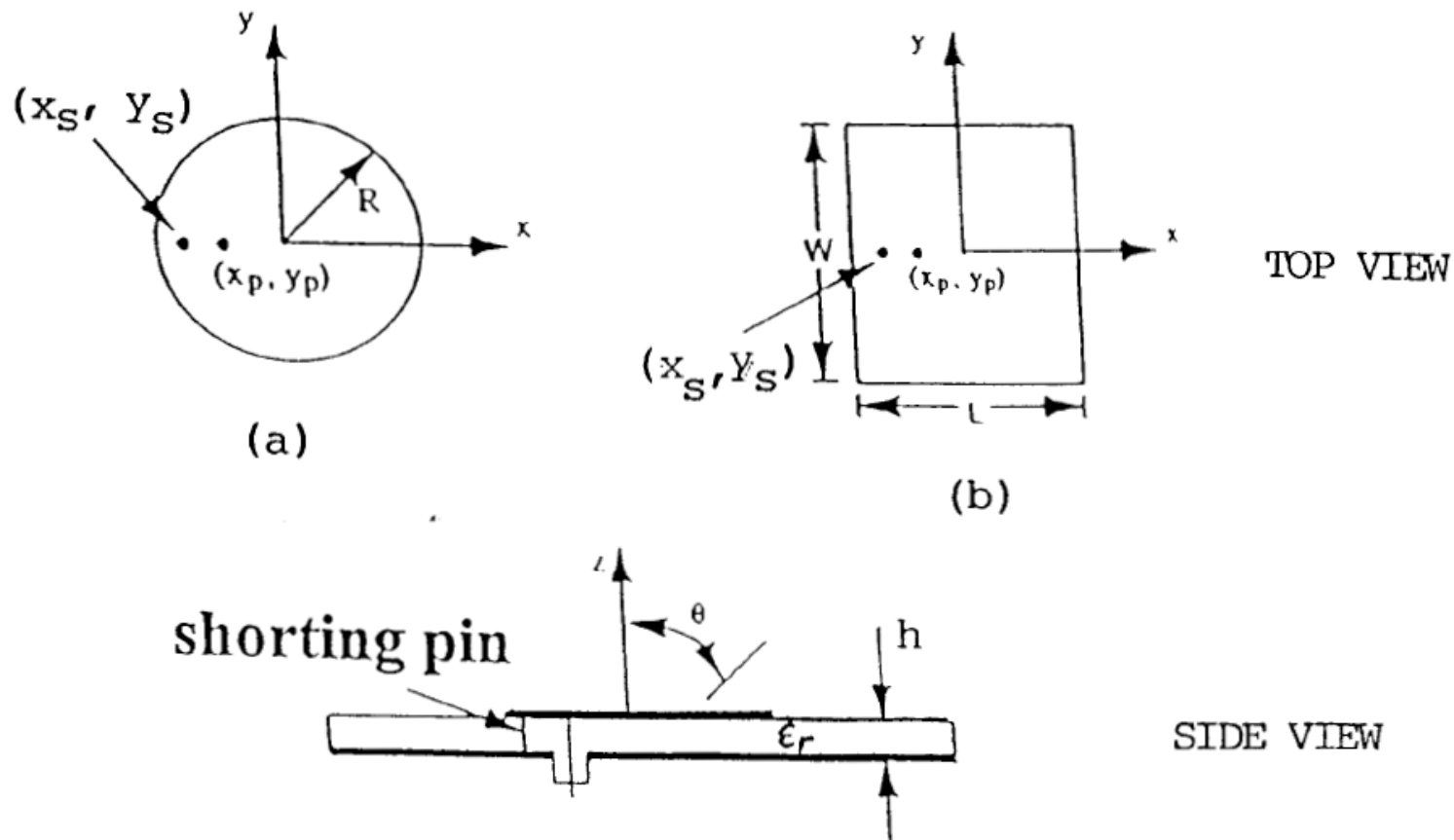


Fig. 4.18 Circular (a) and rectangular (b) patches with shorting post.

10.3 Use of Shorting Pin

- Figure 4.19 shows a circular patch with one shorting pin on foam substrate. Using IE3D simulation software, for the dimensions given in the figure the results for the return loss given by the solid curve of Fig.4.20. The radius of the patch is reduced by a factor of 3 and the area by a factor of 9 when compared to the case of no shorting pin. The thickness of the foam substrate is $0.06 \lambda_0$, and the impedance bandwidth is about 6.3 %. The simulated radiation patterns at 1.9 GHz are shown in Figure 4.21. As noted earlier, the cross polarization of this type of antenna is very high. The simulation results are consistent with the experiments of Waterhouse et al. (1998).
- The bandwidth can be improved using multiple shorting pins. A circular patch with two and three shorting pins are shown in Figs. 4.22 (a) and 4.22 (b). The simulated return loss for these cases are shown in the broken curves of Fig.4.20. The impedance bandwidths are 7.9 % for the patch with 2 pins and 10.0 % for the patch with 3 pins.

10.3 Use of Shorting Pin

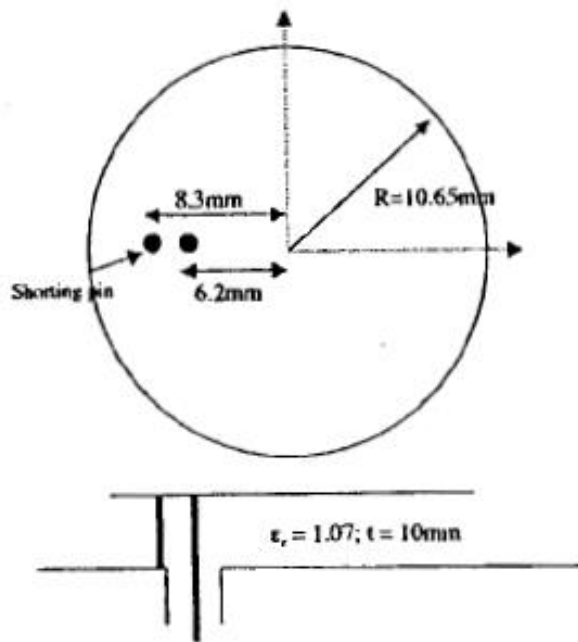


Fig.4.19 Geometry of the circular patch antenna with shorting pin (not to scale).

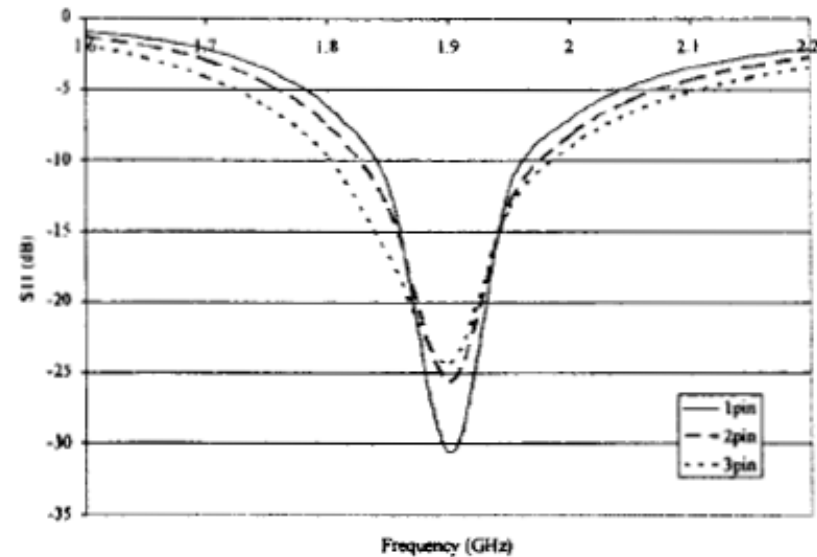


Fig.4.20 Simulated return loss of the miniature patch antenna with different number of shorting pins.

10.3 Use of Shorting Pin

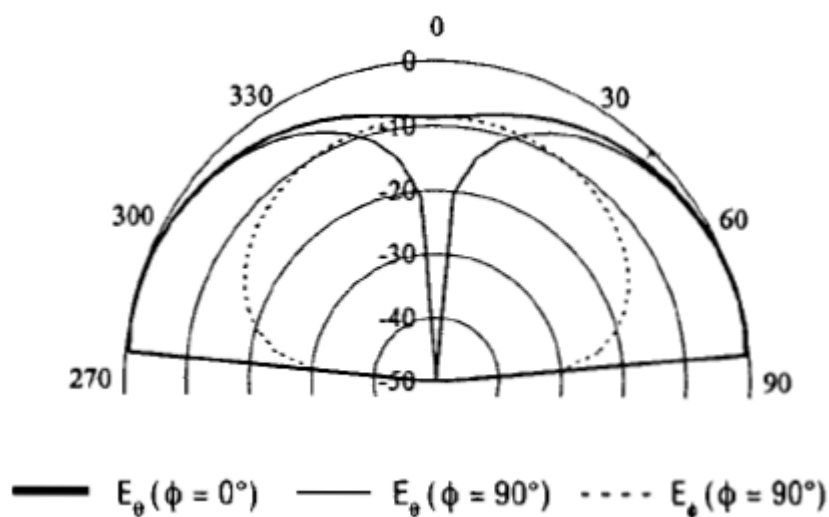
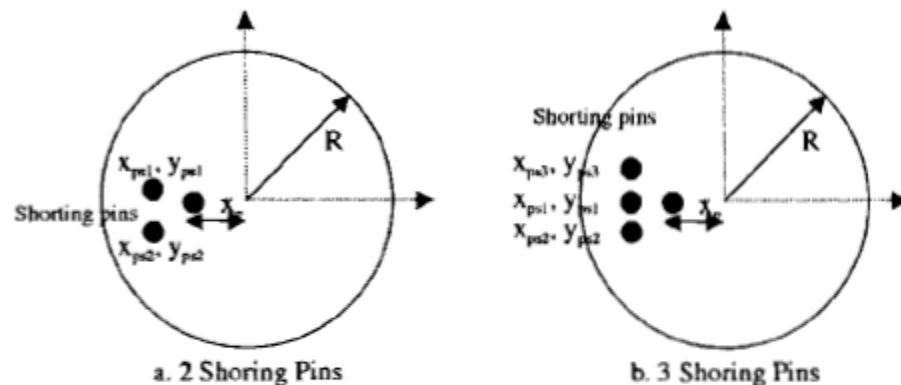


Fig.4.21 Simulated radiation pattern of the miniature patch antenna with 1 shorting pin at 1.9 GHz (10 dB/div).



- a. $R = 13.2$, $x_p = 4.95$, $x_{ps1} = x_{ps2} = 11.08$, $y_{ps1} = 1.95$, $y_{ps2} = -1.95$
 b. $R = 15.4$, $x_p = 2.35$, $x_{ps1} = 13.3$, $x_{ps2} = x_{ps3} = 14.1$, $y_{ps1} = 0$,
 $y_{ps2} = 5.13$, $y_{ps3} = -5.13$

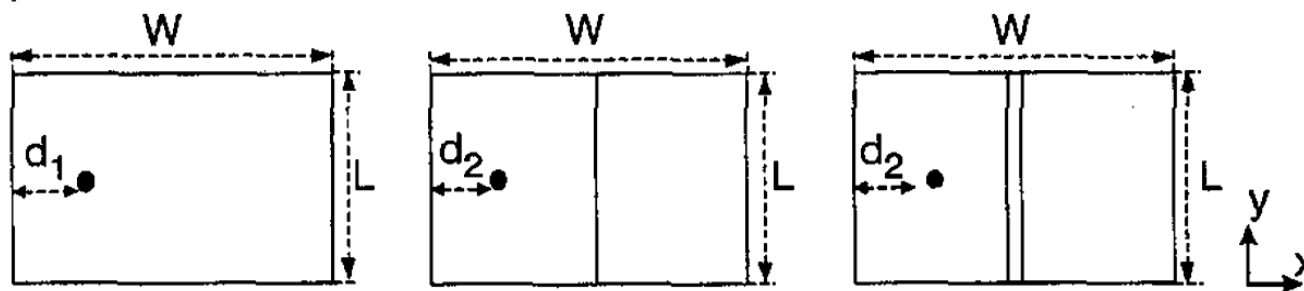
Fig.4.22 Circular patch with 2 and 3 shorting pins (units in mm and not to scale).

10.4 The Folded Patch

- Both the shorting wall and shorting pin size reduction techniques result in high cross polarization levels. A method which maintains a relatively low cross polarization level is that of the folded patch, first introduced by Chair et al. [1998].
- Consider the geometries shown in Fig.4.23. Figure 4.23 (a) presents a conventional patch antenna with length $L = 51$ mm and $W = 31$ mm. The antenna excited in the TM_{10} mode is used as a reference. Figure 4.23 (b) shows a folded patch antenna, designated as folded-patch configuration 1, which is made of a copper sheet of length 85.5 mm and width 31 mm. Figure 4.23 (c) shows a second folded patch antenna, designated as folded-patch configuration 2, which is made of a copper sheet of length 111 mm and width 31 mm. The antennas are fed by coaxial feeds. Although all three antennas have the same length in the top view, it is found that the resonant lengths of the folded patches are effectively longer than the length of the conventional patch.

10.4 The Folded Patch

top view



side view

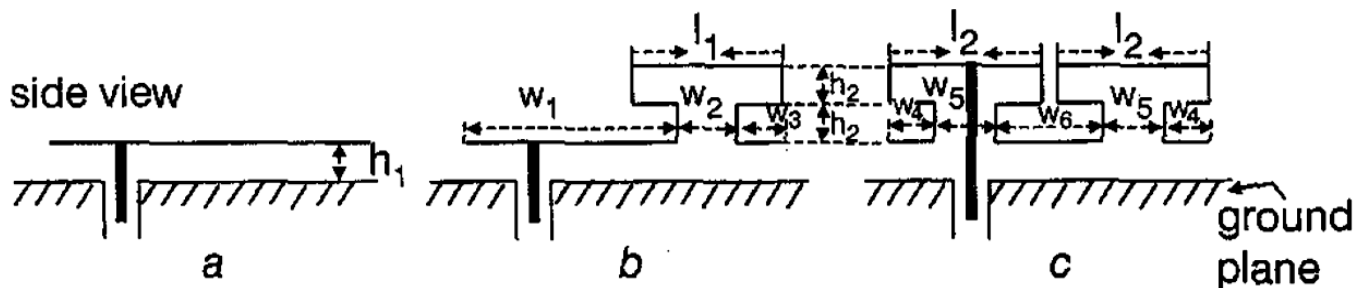
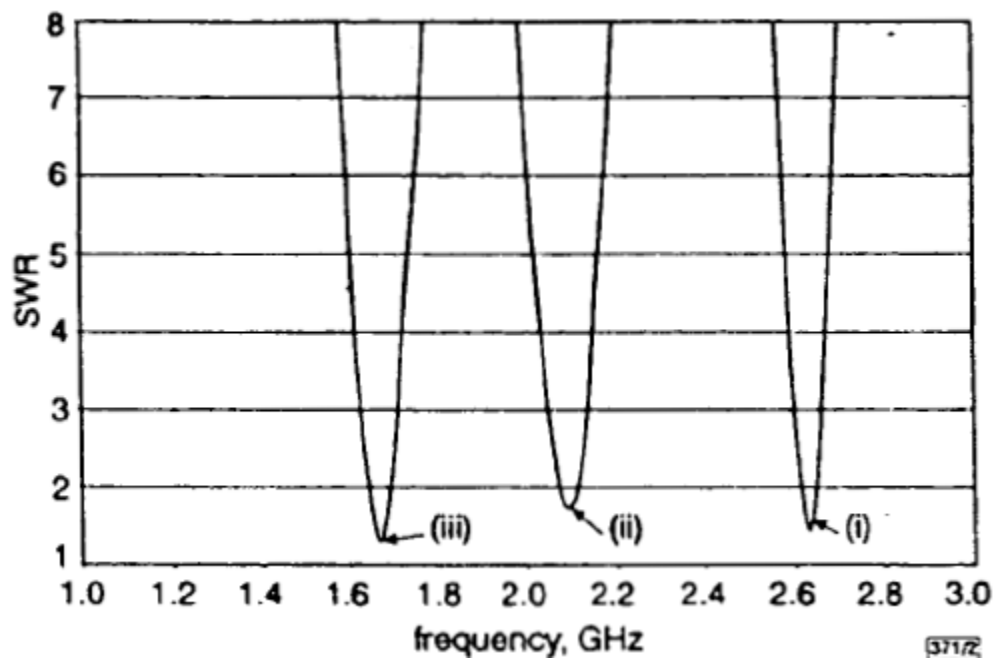


Fig.4.23 Structures of the folded patch antennas.

Prototype: $W=51\text{mm}$, $L=31\text{mm}$, $d_1=20\text{mm}$, $d_2=15\text{mm}$, $h_1=2\text{mm}$, $h_2=3\text{mm}$, $w_1=9.5\text{mm}$, $w_2=5\text{mm}$, $l_1=10\text{mm}$, $l_2=15\text{mm}$, $l_3=15\text{mm}$, $l_4=23\text{mm}$.

10.4 The Folded Patch



- (i) single layer patch; $f_0 = 2.65\text{GHz}$; $BW = 1.23\%$
(ii) folded-patch configuration 1; $f_0 = 2.1\text{GHz}$; $BW = 2.03\%$
(iii) folded-patch configuration 2; $f_0 = 1.66\text{GHz}$; $BW = 3.16\%$

Fig. 4.24 SWR against frequency.

10.4 The Folded Patch

- The measured **SWR** versus frequency of the three antennas are shown in Fig.4.24. The resonant frequency for the conventional patch is 2.65 GHz. Folded-patch configuration 1 has a resonant frequency of 2.1 GHz (20.75 % decrease) while that of folded-patch configuration 2 is 1.66 GHz (37.26 % decrease). The gains of the two configurations are 6.1 and 5.8 dBi, respectively (Fig.4.25), and are larger than the quarter wave shorted patch.
- The radiation patterns of the folded patch configurations have been measured at 2.1 and 1.66 GHz, respectively, and are shown in Figs. 4.26 and 4.27. The co-polarization patterns have maxima in the broadside direction. The cross polarization maximum is -20 dB below the co-polarization maximum. This is significantly lower than that of a shorted quarter-wave patch or patch with shorting pin.

10.4 The Folded Patch

- The impedance bandwidths of the conventional patch and the 2 folded-patches are 1.23 %, 2.03 %, and 3.16 %, respectively. Wider bandwidth folded patches are discussed in Chair et al [1999, 2000].

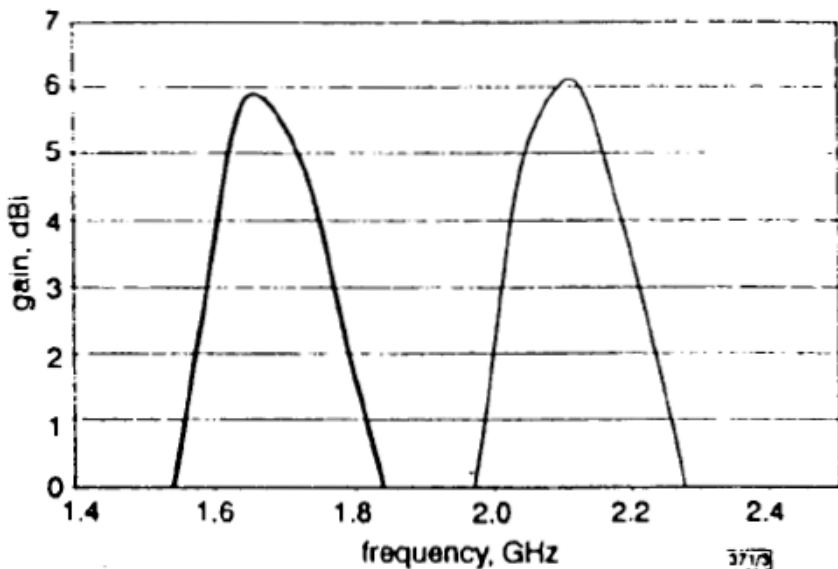


Fig. 4.25 Measured gain.

— configuration 1
 - - - configuration 2

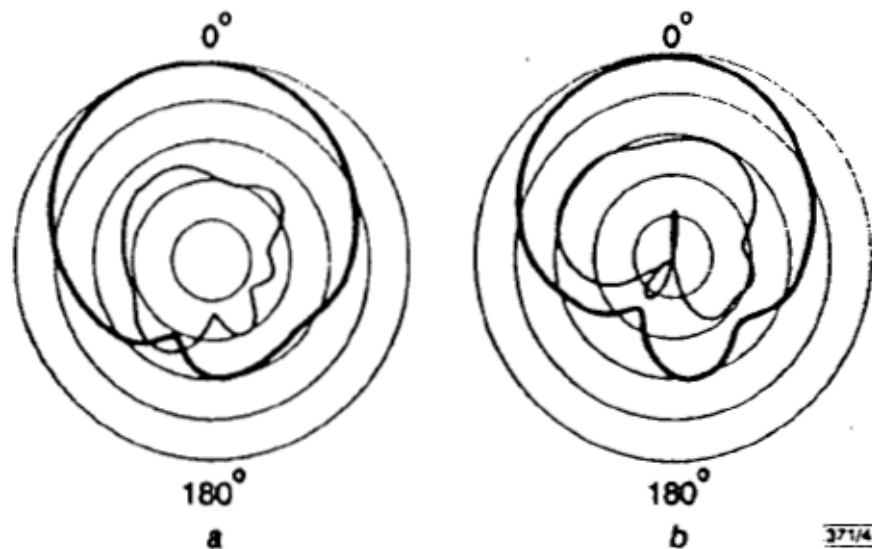


Fig.4.26 Folded-patch configuration 1 radiation pattern.

a E-plane
b H-plane
 — co-polarisation
 - - - cross-polarisation
 10dB/div

10.4 The Folded Patch

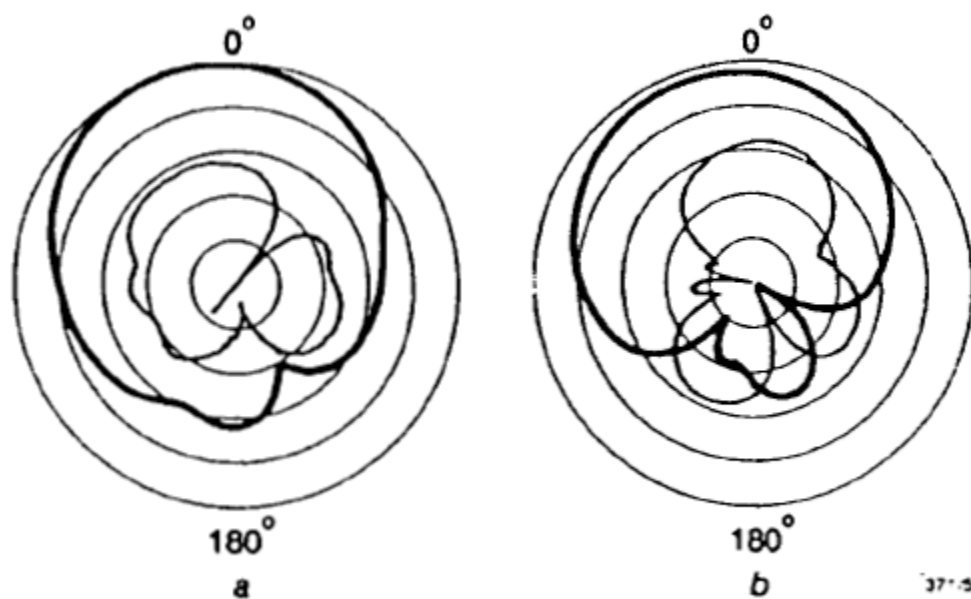


Fig. 4.27 Folded-patch configuration 2 radiation pattern..

a E-plane
b H-plane
— co-polarisation
— cross-polarisation
10dB/div

10.5 Small-Size Wide-Bandwidth Patch Antennas

- The broadbanding techniques discussed previously (U-slot, L-probe, stacked patches) can be combined with the size reduction techniques (shorting wall, shorting pin, folded patch) to obtain small-size patch antennas exceeding 20 % impedance bandwidth. A detailed report of this topic can be found in the review paper by Shackelford et al. [2003].
- The shorting wall technique has also been applied to reduce the size of a dual frequency slot-loaded patch [Guo et al. 2000].

10.6 Comment on ground plane size effect

- Although the ground plane of small antennas usually occupy most of the overall size and their sizes play a significant role, there seems to be little quantitative information on the effect of ground plane size on small patch antennas.
- Recently, a study was made [Tong et al. 2011] on how the size of the ground plane affects the performance of two size-reduced patch antennas, namely, the shorting-wall rectangular patch antenna and the shorting-pin circular patch antenna.
- The results show that, when the ground plane is reduced to less than 30% of the free space wavelength, the performance of the antenna starts to deteriorate. The degree of deterioration varies for the two antennas.
- The ground plane size effects are complicated, dependent on the particular antenna and the locations of the antenna and the feed.

References for size reduction techniques

- ❑ S. Pinhas and S. Shtrikman, "Comparison between computed and measured bandwidth of quarter-wave microstrip radiators," *IEEE Trans. Antennas and Propagation*, Vol. 36(11), pp. 1615-1616, 1988.
- ❑ R. Chair, K. F. Lee and K. M. Luk, "Bandwidth and cross-polarization characteristics of quarter-wave shorted patch antenna," *Microwave and Optical Technology Letters*, Vol. 22, No. 2, pp. 101-103, 1999.
- ❑ K. F. Lee, Y. X. Guo, J. A. Hawkins, R. Chair and K. M. Luk, "Theory and experiment on microstrip patch antennas with shorting walls," *IEE Proc.-Microwave, Antennas and Propagation*, Vol. 147, No. 6, pp. 521-525, 2000.
- ❑ R. B. Waterhouse, S. D. Targonski, and D. M. Kokotoff, "Design and performance of small printed antennas," *IEEE Transactions on Antennas and Propagation*, Vol. 46, No. 11, pp. 1629-1633, 1998.
- ❑ K. M. Luk, R. Chair and K. F. Lee, "Small rectangular patch antenna," *Electronics Letters*, Vol. 34, pp. 2366-2367, 1998.
- ❑ R. Chair, K. M. Luk and K. F. Lee, "Novel miniature shorted dual patch antenna," *IEE Proceedings-Microwave, Antennas and Propagation*, Vol. 137, pp. 273-276, 2000.

- ❑ A. Shackelford, K. F. Lee and K. M. Luk, “Design of small-size wide-bandwidth microstrip patch antennas,” *IEEE Antennas and Propagation Magazine*, Vol. 45, No. 1, pp. 75-83, February 2003.
- ❑ H. Wong, K. M. Luk, C. H. Chan, Q. Xue, K. K. So and H. W. Lai, “Small antennas in wireless communication,” *IEEE Proceedings*, Vol. 100, No. 7, pp. 2109-2121, 2012.
- ❑ Y. X. Guo, A. Shackelford, K. F. Lee, and K. M. Luk, “Broadband quarter-Patch antenna with a U-shaped slot,” *Microwave and Optical Technology Letters*, Vol. 28, pp. 328-330, 2001.
- ❑ A. K. Shackelford, K. F. Lee, K. M. Luk and R. Chair, “U-slot patch antenna with shorting pin,” *Electronics Letters*, Vol. 37, No. 12, pp. 729-730, June 2001.
- ❑ L. Zaid, G. Kossiavas, J-Y Dauvignac, J. Cazajous, and A. Papiernik, “Dual-Frequency and broad-band antennas with stacked quarter wavelength elements,” *IEEE Transactions on Antennas and Propagation*, Vol. 47, No. 4, pp. 654-660, 1999.

- ❑ R. B. Waterhouse, J. T. Rowley, and K. H. Joyner, “Stacked shorted patch,” *Electronics Letters*, Vol. 34, pp. 612-614, 1998.
- ❑ R. B. Waterhouse, “Stacked shorted patch antenna,” *Electronics Letters*, Vol. 35, No. 2, pp. 98-100, 1999.
- ❑ A. A. Deshmukh and G. Kumar, “Half U-slot loaded rectangular microstrip antenna,” in IEEE AP-S Int. Symp. USNC/CNC/URSI National Radio Science Meeting, Vol. 2, pp. 876-879, 2003.
- ❑ C. L. Mak, R. Chair, K. F. Lee, K. M. Luk and A. A. Kishk, “Half U-Slot patch antenna with shorting wall,” *Electronics Letters*, Vol. 39, No. 25, pp.1779-1780, December 2003.
- ❑ R. Chair, K. F. Lee, C. L. Mak, K. M. Luk and A. A. Kishk, “Miniature Wideband Half U-Slot and Half E-Shaped Patch Antennas,” *IEEE Transactions on Antennas and Propagation*, Vol. 53, No. 8, pp. 2645-2652, August 2005.
- ❑ Y. X. Guo, K. M. Luk, and K. F. Lee, “Dual-band slot-loaded short circuited patch antenna,” *Electron. Lett.*, Vol. 36, pp. 289-291, 2000.
- ❑ K. F. Tong, K. F. Lee and K. M. Luk, “On the effect of ground plane size on wideband shorting-wall probe-fed patch antennas,” Proc. Of 2011 ICEAA-IEEE APWC, Torino, Italy.

11. Concluding Remarks and Some Citation Data

In these lectures, I have presented a personal overview of my involvement in the development of patch antennas, starting from the early 1980's, when these antennas began to attract the attention of the antenna community. As you have seen, many of the results were from the collaboration with Prof. Luk and his students, which began when he joined City Polytechnic in 1985, until my retirement in 2011, slightly more than a quarter of a century. We were fortunate to enter the field when it was still at the beginning of its development.

It is perhaps fitting to ask whether our contributions have had an impact in the field. One way of assessing this is to look at the citations of our work in the literature. I have compiled some data from Google Scholar, as Google Scholar is much easier to work with compared with SCI or Scopus.

16 Papers on Patch Antennas by K. F. Lee and collaborators have, according to Google Scholars, been cited more than 100 times (as of 10/30/15). Books are excluded. These are shown in the next slide. Note that Prof. Luk is in 10 of the 16 papers.

The 16 papers cover the areas of broadbanding, basic studies, reconfigurable patch antennas, size reduction, dual/triple band designs, and circular polarization.

Title, Authors, Journal	No. of citations	Area
Single-layer single-patch wideband microstrip antenna, T. Huynh, K. F. Lee, Electronics Letters, 31(16), 1310-1312, 1995	574	Broadbanding
Experimental and simulation studies of the coaxially fed U-slot rectangular patch antenna K. F. Lee, K. M. Luk, K. F. Tong, S. M. Shum, T. Huynh, R. Q. Lee, IEE MAP, 144(5), 354-358, 1997	352	Broadbanding
Broadband microstrip patch antenna, K. M. Luk, C. L. Mak, Y. L. Chow, K. F. Lee, Electronics Letters 34(15), 1442-1443, 1998	287	Broadbanding
Characteristics of a two-layer electromagnetically coupled rectangular patch antenna, R. Q. Lee, K. F. Lee, J. Bobinchak, Electronics Letters 23(20), 1070-1072, 1987	273	Broadbanding
Experimental study of a microstrip patch antenna with an L-shaped probe, C. L. Mak, K. M. Luk, K. F. Lee, Y. L. Chow, IEEE Transactions on Antennas and Propagation, 48(5), 777-783, 2000	248	Broadbanding
A broad-band U-slot rectangular patch antenna on a microwave substrate, K. F. Tong, K. M. Luk, K. F. Lee, R. Q. Lee, IEEE Transactions on Antennas and Propagation, 48(6), 954-960, 2000	196	Broadbanding
Analysis of the cylindrical-rectangular patch antenna, K. M. Luk, K. F. Lee, J. S. Dahele, IEEE Transactions on Antennas and Propagation, 37(2), 143-147, 1989	162	Basic Studies
Design of small-size wide-bandwidth microstrip patch antennas, A. K. Shackelford, K. F. Lee, K. M. Luk, IEEE Antennas and Propagation Magazine, 45(1), 75-83, 2003	156	Size Reduction

Title, Authors, Journal	No. of citations	Area
Analysis and design of L-probe proximity fed-patch antennas, Y. X. Guo, C. L. Mak, K. M. Luk, K. F. Lee, IEEE Transactions on Antennas and Propagation, 49(2) 145-149, 2001	151	Broadbanding
Experimental study of the two-layer electromagnetically coupled rectangular patch antenna, R. Q. Lee, K. F. Lee, IEEE Transactions on Antennas and Propagation, 38(8), 1298-1302, 1990	151	Broadbanding
Dual-frequency stacked annular-ring microstrip antenna, J. S. Dahele, K. F. Lee, D. Wong, IEEE Transactions on Antennas and propagation, 35(11), 1281-1285, 1987	142	Dual frequency design
Design and study of wideband single feed circularly polarized microstrip antenna, S.L.S. Yang, K. F. Lee, A. A. Kishk, K. M. Luk, Progress in Electromagnetics Research, 80, 45-61, 2008	130	Circular polarization
Characteristics of the equilateral triangular patch antenna, K. F. Lee, K. M. Luk, J. S. Dahele, IEEE Transactions on Antennas and Propagation, 36(11), 1510-1518, 1988.	115	Basic studies
Double U-slot rectangular patch antenna, Y. X. Guo, K. M. Luk, K. F. Lee, Y. L. Chow, Electronics Letters, 34(19), 1805-1806, 1982.	112	Broadbanding
Theory and experiment on microstrip antennas with airgaps, J. S. Dahele, K. F. Lee, IEE Proceedings H (Microwaves, Antennas and propagation), 132(7), 455-460, 1985.	111	Reconfigurable Patch antennas
Circular-disk microstrip antenna with an air gap, K. F. Lee, K. Y. Ho, J. S. Dahele, IEEE Transactions on Antennas and Propagation, 32(8), 880-884, 1984.	104	Reconfigurable patch antennas

Papers with > 100 citations grouped according to topic

Topic	Number of Citations as of 10/30/2015
Broadbanding	2,344
Basic studies (air gap papers classified as reconfigurable)	277
*Reconfigurable	215
Size reduction	156
*Dual/triple band	142
*Circular polarization	130
Total for 16 papers	3,264

(*Some relatively recent papers in the categories of reconfigurable, dual/triple band and circular polarization are rapidly reaching 100 citations. They are not included in this table.)